LETTERS

Suppression of Myc oncogenic activity by ribosomal protein haploinsufficiency

Maria Barna[1], Aya Pusic[2]*, Ornella Zollo[2]*, Maria Costa[2], Nadya Kondrashov[1], Eduardo Rego[3], Pulivarthi H. Rao[4] & Davide Ruggero[2]

The *Myc* oncogene regulates the expression of several components of the protein synthetic machinery, including ribosomal proteins, initiation factors of translation, RNA polymerase III and ribosomal DNA[1,2]. Whether and how increasing the cellular protein synthesis capacity affects the multistep process leading to cancer remains to be addressed. Here we use ribosomal protein heterozygote mice as a genetic tool to restore increased protein synthesis in *Eμ-Myc*/+ transgenic mice to normal levels, and show that the oncogenic potential of Myc in this context is suppressed. Our findings demonstrate that the ability of Myc to increase protein synthesis directly augments cell size and is sufficient to accelerate cell cycle progression independently of known cell cycle targets transcriptionally regulated by Myc. In addition, when protein synthesis is restored to normal levels, Myc-overexpressing precancerous cells are more efficiently eliminated by programmed cell death. Our findings reveal a new mechanism that links increases in general protein synthesis rates downstream of an oncogenic signal to a specific molecular impairment in the modality of translation initiation used to regulate the expression of selective messenger RNAs. We show that an aberrant increase in cap-dependent translation downstream of Myc hyperactivation specifically impairs the translational switch to internal ribosomal entry site (IRES)-dependent translation that is required for accurate mitotic progression. Failure of this translational switch results in reduced mitotic-specific expression of the endogenous IRES-dependent form of Cdk11 (also known as Cdc2l and PITSLRE)[3–5], which leads to cytokinesis defects and is associated with increased centrosome numbers and genome instability in *Eμ-Myc*/+ mice. When accurate translational control is re-established in *Eμ-Myc*/+ mice, genome instability is suppressed. Our findings demonstrate how perturbations in translational control provide a highly specific outcome for gene expression, genome stability and cancer initiation that have important implications for understanding the molecular mechanism of cancer formation at the post-genomic level.

Deregulation of Myc activity is one of the most frequent oncogenic lesions underlying human cancers[6,7]. Myc has an evolutionarily conserved role in the control of cell size and protein synthesis rates, which in *Drosophila* confers a cell survival advantage[1,8,9]. When dMyc-induced protein synthesis is restrained in a *minute* mutant background, which is haploinsufficient for ribosomal protein function, cells no longer possess a competitive advantage[10,11]. So far, the relevance of Myc-dependent increases in protein synthesis and cell growth in the multistep process leading to cancer remain unknown.

To restore protein synthesis rates in Myc-overexpressing cells to normal, we used mouse *minute* mutants that are haploinsufficient for ribosomal protein function. Haploinsufficiency in certain ribosomal proteins decreases the overall protein synthesis rates to an extent that is compatible with overall cellular and tissue homeostasis. $L24^{+/-}$ mice are viable[12] and do not show any overt differences in B-lymphocyte development, growth and cell division (Fig. 1 and

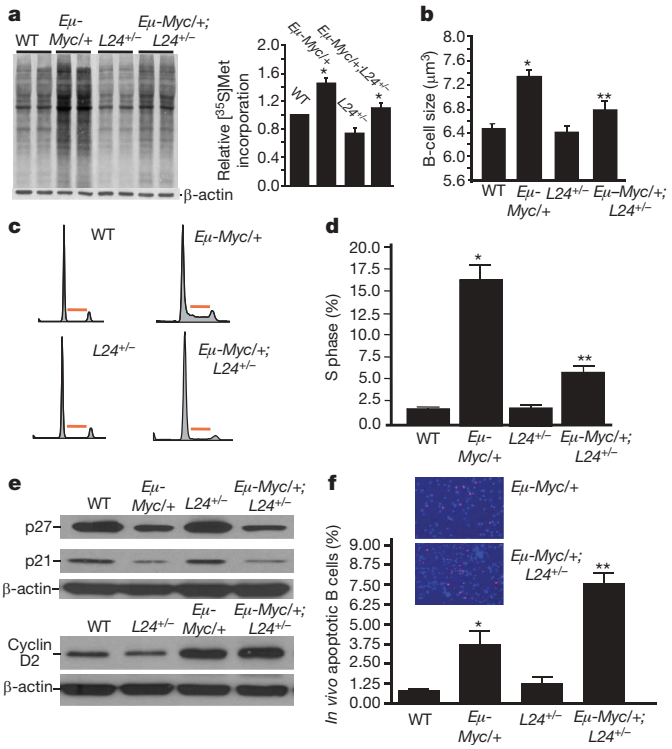

Figure 1 | Myc-induced increases in protein synthesis regulates B-lymphocyte size, division and apoptosis before lymphomagenesis. **a**, Protein synthesis rates assessed by [^{35}S] methionine incorporation and densitometry analysis; $^{*}P < 0.01$; $n = 3$. **b**, Cell size analysis; $n = 3$, $^{*}P < 0.001$ for *Eμ-Myc*/+ versus wild type (WT), $^{**}P < 0.01$ for *Eμ-Myc*/+ versus *Eμ-Myc*/+;$L24^{+/-}$. **c**, **d**, Cell cycle distribution (**c**) and quantification of the percentage of cells in S phase (**d**); $n = 3$; $^{*}P < 0.01$, $^{**}P < 0.05$. The red bar in **c** indicates S phase. **e**, Western blot analysis for cell cycle targets transcriptionally regulated by Myc. **f**, *In situ* TUNEL analysis; $n = 3$. Insets (original magnification ×20) are representative pictures of TUNEL analysis comparing *Eμ-Myc*/+ and *Eμ-Myc*/+;$L24^{+/-}$ samples; $^{*}P < 0.05$, $^{**}P < 0.05$. All experiments (**a**–**e**) were performed on freshly isolated B-lymphocytes. Error bars, s.d.

[1]Department of Biochemistry & Biophysics, University of California San Francisco, Rock Hall Room 384C, 1550 Fourth Street, San Francisco, California 94158-2517, USA. [2]School of Medicine and Department of Urology, Helen Diller Family Comprehensive Cancer Center, University of California San Francisco, Byers Hall Room 308E, 1700 Fourth Street, San Francisco, California 94158-2517, USA. [3]Center for Cell Based Therapy, Fundação Hemocentro de Ribeirão Preto, University of Sao Paulo, 14048-900 Brazil. [4]Department of Pediatrics, Baylor College of Medicine, Houston, Texas 77030, USA.
*These authors contributed equally to this work.

Supplementary Fig. 1). We intercrossed Myc transgenic mice, in which Myc is overexpressed in the B-cell compartment (*Eμ-Myc/+*)[13], with $L24^{+/-}$ mice (Supplementary Fig. 2). By lowering the threshold of protein production in $L24^{+/-}$ mice, the increased protein synthesis rates and cell size in *Eμ-Myc/+* cells[14] were restored to normal levels in *Eμ-Myc/+*;$L24^{+/-}$ mice (Fig. 1a, b). Therefore, this genetic approach shows that Myc-induced increases in general protein synthesis rates are responsible for augmented cell growth. Moreover, *Eμ-Myc/+*;$L24^{+/-}$ mice are an important genetic model for selectively rescuing increased protein synthesis rates and cell growth downstream of oncogenic Myc signalling.

During cell cycle progression, cell growth normally precedes cell division and it has been suggested that cells must reach a critical cell size or 'setpoint' to facilitate G1–S progression[15]. In mammalian cells, it remains undetermined whether an increase in cell growth is coupled to an increase in cell division upon Myc hyperactivation. The percentage of *Eμ-Myc/+* cells in S phase is markedly increased compared to wild-type cells (Fig. 1c, d). Notably, in *Eμ-Myc/+*;$L24^{+/-}$ mice the augmented number of cells in S phase is restored to normal levels (Fig. 1c, d). The rate of cell cycle progression in *Eμ-Myc/+* B-lymphocytes was also monitored by BrdU incorporation ($BrdU^+$ cells per h, wild-type 0.16 ± 0.04 versus Myc 5.77 ± 1.78, $P < 0.005$) and was similarly restored to normal levels in *Eμ-Myc/+*;$L24^{+/-}$ cells ($BrdU^+$ cells per h, 0.11 ± 0.02, $P < 0.02$). Important cell cycle targets that are transcriptionally regulated by Myc such as p27 (also known as Cdkn1b; ref. 16), p21 (Cdkn1a; ref. 17) and cyclin D2 (Ccnd2; ref. 18), were expressed at similar levels in *Eμ-Myc/+* and *Eμ-Myc/+*;$L24^{+/-}$ cells (Fig. 1e and Supplementary Fig. 3). Thereby, the overall protein synthetic capacity of the cell may dictate cell cycle progression independently from the cell cycle program established at the transcriptional level by Myc hyperactivation. These results strongly suggest that Myc-induced cell growth is dependent on the ability of Myc to regulate protein synthesis and is coupled to uncontrolled cell cycle progression in cancer.

Non-immortalized cells counteract Myc overexpression by undergoing programmed cell death as a tumour suppressive response, and inhibition of cell death downstream of Myc activation accelerates lymphoma initiation[7]. The percentage of dying cells in *Eμ-Myc/+*;$L24^{+/-}$ mice was more than double that of *Eμ-Myc/+* mice before lymphoma onset (Fig. 1f). Therefore, the tumour suppressive response elicited by Myc overexpression is strongly enhanced in the background of normal protein synthesis and these findings suggest that clonal derivatives of precancerous cells may be more efficiently eliminated by programmed cell death in *Eμ-Myc/+*;$L24^{+/-}$ mice.

The restoration of normal protein synthesis downstream of Myc in *Eμ-Myc/+*;$L24^{+/-}$ mice is first associated with a marked reduction in splenomegaly—the earliest manifestation of Myc-induced lymphomagenesis (Fig. 2a). We next scored for lymphoma formation in each cohort of mice (Fig. 2b). The onset of lymphomas in the *Eμ-Myc/+*;$L24^{+/-}$ mice is markedly delayed compared to *Eμ-Myc/+* mice (Fig. 2b). In addition, a significant percentage of *Eμ-Myc/+*;$L24^{+/-}$ mice do not develop lymphomas even after 1.5 years of age (Fig. 2b). A second mouse *minute* line, heterozygous for the ribosomal protein L38 (M.B., manuscript in preparation), was intercrossed with *Eμ-Myc/+* mice. *Eμ-Myc/+*;$L38^{+/-}$ mice also show a marked rescue in cell growth and cell division as well as an increase in cell death of precancerous cells compared to *Eμ-Myc/+* cells (Supplementary Figs 1 and 4). Notably, lymphoma initiation in the *Eμ-Myc/+*;$L38^{+/-}$ mice was markedly suppressed, as in the *Eμ-Myc/+*;$L24^{+/-}$ mice (Supplementary Fig. 5). The suppression of lymphomagenesis was specific to the direct effect of Myc signalling on protein synthesis, as ribosomal protein haploinsufficiency in the context of the $p53^{-/-}$ background did not have any effect on tumour formation (Fig. 2c). These genetic results demonstrate that the ability of Myc to augment protein synthesis is necessary for its oncogenic potential.

To understand further the molecular mechanisms by which unrestrained increases in global protein synthesis can lead to tumorigenesis, we analysed protein synthesis control during specific phases of the cell cycle in *Eμ-Myc/+* B-lymphocytes. Unexpectedly, wild-type and *Eμ-Myc/+* cells synchronized in S phase did not show any differences in protein synthesis rates (Fig. 3a). During mitosis, cap-dependent protein synthesis is normally decreased to facilitate cap-independent translation of a subset of messenger RNAs required for accurate mitotic progression[19]. On the contrary, *Eμ-Myc/+* cells show increased protein synthesis rates during mitosis; this is cap-dependent as the increased protein synthesis rates are restored to normal levels after rapamycin treatment (Supplementary Fig. 6) and in *Eμ-Myc/+*;$L24^{+/-}$ cells (Fig. 3a, b). Moreover, increased activity of a cap-dependent luciferase reporter gene is observed in Myc-overexpressing cells synchronized in mitosis and this is restored to normal when Myc is overexpressed in the $L24^{+/-}$ background (Fig. 3c).

Accurate mitotic progression relies on a very precise and orderly switch in translational control through a general decrease in cap-dependent translation and a switch to IRES-dependent translation initiation[19]. We next addressed whether a persistent enhancement of cap-dependent translation during mitosis downstream of Myc overexpression would be unfavourable to an IRES-dependent translational switch. The expression of a bicistronic reporter construct harbouring the hepatitis C virus IRES element (HCV IRES)—a molecular readout of IRES-dependent translation[20]—is impaired in mitotically synchronized Myc-overexpressing cells and restored to normal when Myc is overexpressed in the $L24^{+/-}$ background (Fig. 3d). Notably, $L24^{+/-}$ cells do not show differences in IRES-dependent translation

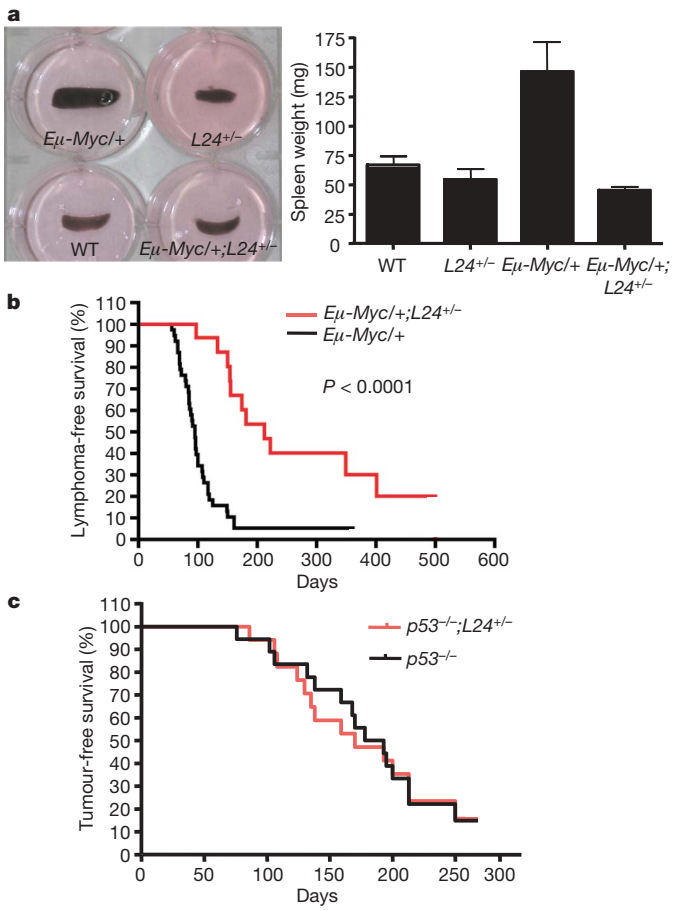

Figure 2 | The ability of Myc to augment protein synthesis is necessary for its oncogenic potential. **a**, Representative photographs of spleens (left) and average spleen weight (right); WT, wild type; $n = 6$ per genotype, 4 weeks of age; error bars, s.d. **b**, Kaplan–Meier curves showing lymphoma-free survival of *Eμ-Myc/+* and *Eμ-Myc/+*;$L24^{+/-}$ mice; $n = 30$ per genotype. **c**, Kaplan–Meier curves showing tumour-free survival of $p53^{-/-}$ and $p53^{-/-}$;$L24^{+/-}$ mice; $n = 25$ per genotype.

compared to wild-type cells (Fig. 3d), suggesting that the rescue in IRES-dependent translation downstream of Myc hyperactivation in the $L24^{+/-}$ background is the result of restoring cap-dependent translation to normal levels (Fig. 3c). Taken together, these data demonstrate that aberrant and continuous stimulation of cap-dependent protein synthesis by Myc perturbs the mitotic switch to IRES-dependent translation.

We next monitored the expression of a well-characterized endogenous mRNA that is only translated during mitosis by an IRES element. *Cdk11* (also known as Cdc2l and PITSLRE) is a member of the Cdc2-like protein kinase family that undergoes cap-independent translation from an IRES element during mitosis to produce a 58-kDa Cdk11 isoform, $Cdk11^{p58}$, that facilitates accurate mitotic progression[3,4]. Notably, deletions containing the *Cdk11* locus are found in non-Hodgkin's lymphoma[21] and other cancers[22,23], strongly suggesting that Cdk11 may act as a tumour suppressor gene[24]. The expression of $Cdk11^{p58}$ was markedly reduced in mitotically synchronized *Eμ-Myc/+* cells (Fig. 3e and Supplementary Fig. 7) but was rescued to normal levels in *Eμ-Myc/+;L24*$^{+/-}$ cells (Fig. 3e). Moreover, expression of a reporter gene directed by the $Cdk11^{p58}$ IRES element is also impaired in mitotically synchronized Myc-overexpressed cells and restored to normal levels when Myc is overexpressed in the $L24^{+/-}$ background (Fig. 3f). These findings indicate that the general increase in cap-dependent translation downstream of Myc activation prevents the accurate mitotic switch to IRES-dependent translation that regulates $Cdk11^{p58}$ expression.

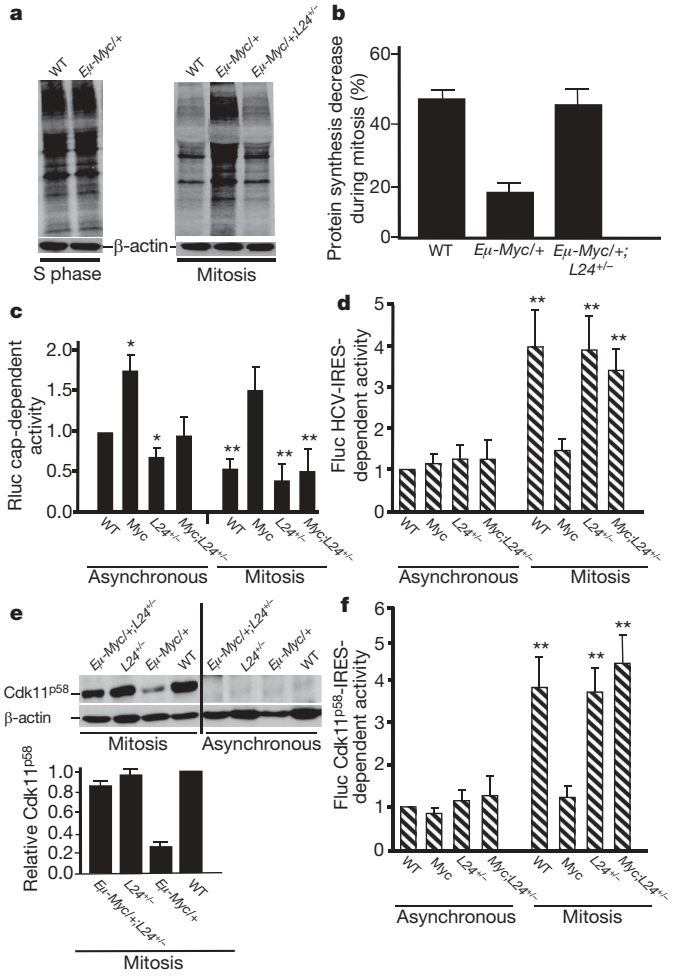

Figure 3 | Myc hyperactivation impairs the translational switch from cap- to IRES-dependent translation control during mitosis and blocks mitotic translation of the Cdk11 kinase. **a**, **b**, [^{35}S]methionine incorporation in B lymphocytes synchronized in S phase and mitosis. Densitometry analysis ($n = 3$) comparing protein synthesis levels in S phase and mitotically arrested B lymphocytes is shown. **c**, Cap-dependent activity of the *Renilla* luciferase (Rluc) reporter mRNA in asynchronous and mitotically synchronized MEFs; $n = 6$ experiments performed in triplicate, $^{*}P < 0.001$ compared to wild type (WT), $^{**}P < 0.005$ compared to asynchronous values. **d**, HCV-IRES-dependent activity of the Firefly luciferase (Fluc) reporter mRNA; $n = 6$ experiments performed in triplicate in asynchronous and mitotically synchronized MEFs; $^{**}P < 0.001$ compared to asynchronous values. **e**, Representative western blot of the endogenous $Cdk11^{p58}$ kinase in asynchronous and mitotically synchronized primary B lymphocytes. Note that expression of $Cdk11^{p58}$ is only present in mitotically synchronized cells (left), and not asynchronous cells (right) via an IRES-element positioned in its 5′UTR. Densitometric analysis is shown at the bottom; $n = 3$. **f**, $Cdk11^{p58}$-IRES-dependent activity of firefly luciferase reporter mRNA transfected in asynchronous and mitotically synchronized cells; $n = 4$ experiments performed in triplicate; $^{**}P < 0.001$ compared to asynchronous values. Average steady state wild-type values in **c**, **d** and **f** were set to 1. The *y*-axes show the fold change. Error bars, s.d. A tamoxifen-inducible Myc vector was expressed in a wild-type and L24$^{+/-}$ background in **c**, **d** and **f**.

Decreased $Cdk11^{p58}$ expression during mitosis impairs accurate cytokinesis, resulting in a binucleated cell phenotype[5] that is associated with aneuploidy[25]. We observed that Myc-overexpressing mouse embryonic fibroblasts (MEFs) display cytokinesis defects and have a significant increase in the number of binucleated cells, a hallmark of $Cdk11^{p58}$ loss of function[5] (Fig. 4a). Notably, restoring accurate mitotic $Cdk11^{p58}$ expression in Myc-overexpressing cells was sufficient to revert all of these cytokinesis defects (Fig. 4a–c). These findings strongly suggest that the decreased IRES-dependent translation of $Cdk11^{p58}$ downstream of oncogenic Myc signalling may be an early event in tumorigenesis that underlies the subsequent development of genomic instability[26].

We therefore assessed whether *Eμ-Myc/+* lymphocytes have supernumerary centrosomes, an early characteristic of genome instability. We observed a large percentage of *Eμ-Myc/+* cells showing centrosome duplications. These duplications are the result of aberrant protein synthesis control downstream of Myc activation because *Eμ-Myc/+;L24*$^{+/-}$ cells show normal centrosome numbers (Fig. 4d). We next directly monitored genomic instability by using comparative genomic hybridization (CGH) analysis. All of the lymphomas analysed from *Eμ-Myc/+* mice had chromosomal abnormalities, but *Eμ-Myc/+;L24*$^{+/-}$ tumours either showed no chromosomal abnormalities or showed them at a lower frequency (Fig. 4e). These findings establish a direct and previously unrecognized molecular connection between the aberrant control of protein synthesis downstream of Myc activation and the accumulation of genetic lesions in tumours.

In our study, we have used ribosomal protein haploinsufficiency as a genetic tool to restore protein synthesis to normal levels downstream of oncogenic Myc activation. It is worth noting that subsets of ribosomal proteins act as tumour suppressors in Zebrafish[27]. However, *L24*$^{+/-}$ and *L38*$^{+/-}$ mice used in this study do not show cancer susceptibility (D.R., unpublished observations). Our findings provide genetic evidence that increased global protein synthesis downstream of Myc activation is a rate-limiting determinant of cancer initiation, and delineate how deregulations in protein synthesis control confer oncogenic potential (Fig. 4f). This strongly suggests that oncogenic signals may monopolize the translational machinery to elicit cooperative effects on cell growth, cell cycle progression and cell survival (Fig. 4f). Moreover, Myc-overexpressing cells have cytokinesis defects, supernumery centrosomes and genomic instability as a consequence of augmented cap-dependent translation, demonstrating a previously unrecognized molecular connection between aberrant protein synthesis control and genome instability in cancer (Fig. 4f).

We have identified a specific translational impairment as a consequence of increasing protein synthesis downstream of oncogenic signalling (Fig. 4f). The failure to suppress cap-dependent translation during mitosis in Myc-overexpressing cells prevents the critical switch to IRES-dependent translation that is required for accurate

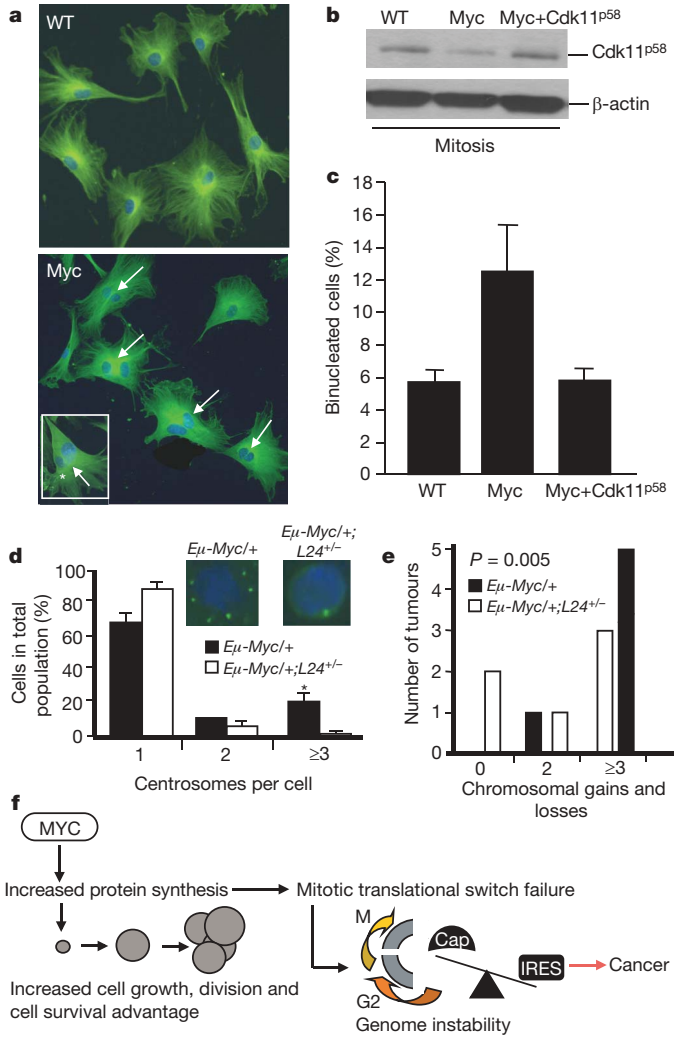

Figure 4 | Aberrant translation control downstream of Myc activation underlies cytokinesis defects and genome instability. a, Myc-overexpressing MEFs (original magnification ×20) show increased numbers of binucleated cells (arrows). Inset (original magnification ×40) illustrates dysmorphic and variably sized nuclei frequently observed in Myc overexpressing MEFs. WT, wild type. **b**, Western blot of mitotic Cdk11^{p58} expression showing decreased expression in MEFs expressing a Myc inducible vector. Myc+p58 cells express a retroviral *Cdk11^{p58}* cDNA. **c**, The increased number of binucleated cells in Myc-overexpressing cells is restored to normal level when Cdk11^{p58} is reintroduced; $n = 4$, at least 500 cells were scored per experiment. Error bars, s.d. **d**, Percentages of cells with normal (1 and 2) and aberrant (3) centrosome numbers in freshly isolated B-lymphocytes; $n = 6$, at least 300 cells per experiment; $^*P < 0.001$. Insets show representative immunofluorescence staining with a centrosome marker. **e**, CGH analysis of tumours; $n = 6$; error bars, s.d. **f**, Proposed model for how deregulations in translation control downstream of Myc activation lead to cancer initiation. Myc-dependent increases in protein synthesis augment cell growth and this effect is coupled to increased cell cycle progression and a cell survival advantage. Increasing cap-dependent translation downstream of Myc-activation also gives rise to a specific molecular impairment in the modality of translation initiation used during mitosis that leads to cytokinesis defects associated with genome instability.

expression of mitotically expressed mRNAs and suggests that many IRES-containing mRNAs, such as *Cdk11*, may be deregulated at the translational level in Myc-overexpressing cells. Defects in the mitotic translational switch are directly relevant for tumorigenesis, as we have shown that impairments in IRES-dependent translation of Cdk11^{p58} result in cytokinesis failure, an early event in cancer that underlies the subsequent development of genomic instability[5,25,28] and which can be reverted in Myc-overexpressing cells by restoring accurate Cdk11^{p58} mitotic expression (Fig. 4a–c). A question remains as to why an increase in cap-dependent translation downstream of Myc activation would decrease IRES-dependent translation. An aberrant increase in cap-dependent translation during mitosis may cause preferential recruitment of translational components (ribosomes and translation initiation factors) to the cap structure at the expense of IRES elements that govern accurate expression of a subset of mRNAs[29]. Several tumour suppressor genes possess an IRES-element and defects in IRES-dependent translation underlie the cancer susceptibility syndrome Dyskeratosis Congenita[30]. Therefore, IRES-containing mRNAs may be preferentially affected as a consequence of deregulations in translational control and may contribute to tumorigenesis. Our data strongly suggest that alterations in quantitative as well as qualitative translational control downstream of oncogenic signalling provide a highly specific and rapid response that may overshadow the effect of the transcriptosome towards cellular transformation.

METHODS SUMMARY

Mice. *Eμ-Myc/+*, *L24*$^{+/-}$, *L38*$^{+/-}$ and *p53*$^{-/-}$ mice were all maintained on a C57/BL6 background. Mice were monitored twice a week for signs of morbidity and tumour development. Myc tumour initiation was scored by peripheral lymph node palpation. Moribund mice or mice with obvious tumours were killed, and tumours and different organs were analysed by histology or processed for further analysis.

Cell culture and analysis of IRES-dependent translation in mitosis. Primary B-lymphocytes were isolated from spleen or bone marrow from 4–5-week-old mice using an autoMACS separator (Miltenyi Biotec). Primary B-lymphocytes and MEFs were synchronized in mitosis by thymidine and aphidicolin block, respectively. Bicistronic vectors, HCV IRES and *Cdk11^{p58}* IRES were transfected as RNAs. IRES-dependent expression of the endogenous Cdk11^{p58} was assessed by western blot using anti-Cdk11^{p58} (Abcam).

Analysis of global protein synthesis. Equal numbers of freshly isolated or cultured primary B-lymphocytes synchronized in S phase or mitosis were incubated in methionine-free DMEM and then 50 μCi per well (25 μCi ml^{-1}) of [^{35}S] methionine was added to the cultures for 35 min. Radiolabelled proteins were visualized by exposure to X-ray film and quantified by densitometry analysis.

Cellular and molecular analysis of B-lymphocytes. Freshly isolated and cultured B-lymphocytes from 4–5-week-old mice were fixed and stained with the following combination of monoclonal antibodies conjugated with fluorescein isothiocyanate (FITC) or phycoerythrin (PE): CD19-PE and CD3-FITC, CD4-PE and CD8-FITC, and CD43-PE and CD45R-B220-FITC. Cell volume measurements were performed using a Coulter Model Z2 (Beckman Coulter).

CGH and cytokinesis analysis. Genomic DNA extracted from lymphomas of *Eμ-Myc/+* and *Eμ-Myc/+;L24*$^{+/-}$ mice was subjected to CGH analysis by standard methods. For cytokinesis analysis, primary MEFs were stably transfected with a Myc-oestrogen receptor chimaera (*MycER*) harbouring puromycin resistance or with *p58* cDNA plus *MycER* via a Phoenix viral vector and cultured. After release from aphidicolin, Myc was activated by the addition of hydroxytamoxifen (OHT). At the 20 h time point, cells were fixed and stained. Binucleated cells were scored used automated segmentation routines.

Full Methods and any associated references are available in the online version of the paper at www.nature.com/nature.

Received 23 July; accepted 16 September 2008.
Published online 16 November 2008.

1. Gomez-Roman, N. *et al.* Activation by c-Myc of transcription by RNA polymerases I, II and III. *Biochem. Soc. Symp.* **73,** 141–154 (2006).
2. Ruggero, D. & Pandolfi, P. P. Does the ribosome translate cancer? *Nature Rev. Cancer* **3,** 179–192 (2003).
3. Cornelis, S. *et al.* Identification and characterization of a novel cell cycle-regulated internal ribosome entry site. *Mol. Cell* **5,** 597–605 (2000).
4. Petretti, C. *et al.* The PITSLRE/CDK11^{p58} protein kinase promotes centrosome maturation and bipolar spindle formation. *EMBO Rep.* **7,** 418–424 (2006).
5. Wilker, E. W. *et al.* 14-3-3σ controls mitotic translation to facilitate cytokinesis. *Nature* **446,** 329–332 (2007).
6. Boxer, L. M. & Dang, C. V. Translocations involving c-*myc* and c-*myc* function. *Oncogene* **20,** 5595–5610 (2001).
7. Pelengaris, S., Khan, M. & Evan, G. c-MYC: more than just a matter of life and death. *Nature Rev. Cancer* **2,** 764–776 (2002).
8. Grewal, S. S., Li, L., Orian, A., Eisenman, R. N. & Edgar, B. A. Myc-dependent regulation of ribosomal RNA synthesis during *Drosophila* development. *Nature Cell Biol.* **7,** 295–302 (2005).

9. Johnston, L. A., Prober, D. A., Edgar, B. A., Eisenman, R. N. & Gallant, P. *Drosophila myc* regulates cellular growth during development. *Cell* **98,** 779–790 (1999).
10. Moreno, E. & Basler, K. dMyc transforms cells into super-competitors. *Cell* **117,** 117–129 (2004).
11. de la Cova, C., Abril, M., Bellosta, P., Gallant, P. & Johnston, L. A. *Drosophila* myc regulates organ size by inducing cell competition. *Cell* **117,** 107–116 (2004).
12. Oliver, E. R., Saunders, T. L., Tarle, S. A. & Glaser, T. Ribosomal protein L24 defect in belly spot and tail (*Bst*), a mouse *Minute*. *Development* **131,** 3907–3920 (2004).
13. Harris, A. W. *et al.* The Eμ-*myc* transgenic mouse. A model for high-incidence spontaneous lymphoma and leukemia of early B cells. *J. Exp. Med.* **167,** 353–371 (1988).
14. Iritani, B. M. & Eisenman, R. N. c-Myc enhances protein synthesis and cell size during B lymphocyte development. *Proc. Natl Acad. Sci. USA* **96,** 13180–13185 (1999).
15. Thomas, G. An encore for ribosome biogenesis in the control of cell proliferation. *Nature Cell Biol.* **2,** E71–E72 (2000).
16. Yang, W. *et al.* Repression of transcription of the $p27^{Kip1}$ cyclin-dependent kinase inhibitor gene by c-Myc. *Oncogene* **20,** 1688–1702 (2001).
17. Wu, S. *et al.* Myc represses differentiation-induced *p21CIP1* expression via Miz-1-dependent interaction with the *p21* core promoter. *Oncogene* **22,** 351–360 (2003).
18. Bouchard, C. *et al.* Direct induction of cyclin D2 by Myc contributes to cell cycle progression and sequestration of p27. *EMBO J.* **18,** 5321–5333 (1999).
19. Pyronnet, S. & Sonenberg, N. Cell-cycle-dependent translational control. *Curr. Opin. Genet. Dev.* **11,** 13–18 (2001).
20. Hellen, C. U. & Sarnow, P. Internal ribosome entry sites in eukaryotic mRNAmolecules. *Genes Dev.* **15,** 1593–1612 (2001).
21. Dave, B. J. *et al.* Deletion of cell division cycle 2-like 1 gene locus on 1p36 in non-Hodgkin lymphoma. *Cancer Genet. Cytogenet.* **108,** 120–126 (1999).
22. Nelson, M. A. *et al.* Abnormalities in the $p34^{cdc2}$-related PITSLRE protein kinase gene complex (CDC2L) on chromosome band 1p36 in melanoma. *Cancer Genet. Cytogenet.* **108,** 91–99 (1999).
23. Lahti, J. M. *et al.* Alterations in the PITSLRE protein kinase gene complex on chromosome 1p36 in childhood neuroblastoma. *Nature Genet.* **7,** 370–375 (1994).
24. Chandramouli, A. *et al.* Haploinsufficiency of the *cdc2l* gene contributes to skin cancer development in mice. *Carcinogenesis* **28,** 2028–2035 (2007).
25. Fujiwara, T. *et al.* Cytokinesis failure generating tetraploids promotes tumorigenesis in *p53*-null cells. *Nature* **437,** 1043–1047 (2005).
26. Wade, M. & Wahl, G. M. c-Myc, genome instability, and tumorigenesis: the devil is in the details. *Curr. Top. Microbiol. Immunol.* **302,** 169–203 (2006).
27. Amsterdam, A. *et al.* Many ribosomal protein genes are cancer genes in zebrafish. *PLoS Biol.* **2,** e139 (2004).
28. Ganem, N. J., Storchova, Z. & Pellman, D. Tetraploidy, aneuploidy and cancer. *Curr. Opin. Genet. Dev.* **17,** 157–162 (2007).
29. Svitkin, Y. V. *et al.* Eukaryotic translation initiation factor 4E availability controls the switch between cap-dependent and internal ribosomal entry site-mediated translation. *Mol. Cell. Biol.* **25,** 10556–10565 (2005).
30. Yoon, A. *et al.* Impaired control of IRES-mediated translation in X-linked dyskeratosis congenita. *Science* **312,** 902–906 (2006).

Supplementary Information is linked to the online version of the paper at www.nature.com/nature.

Acknowledgements We thank F. McCormick, G. Evan and P. O'Farrell for critically reading the manuscript; J. Testa for support and critical discussion during early stages of this work; W. Xu and R. Adamo for technical assistance; J. Copley for editing the manuscript, S. Cornelis for the Cdk11 IRES bicistronic vector. This work was supported by the NIH (D.R.) and the Sandler Foundation (M.B.).

Author Contributions M.B. and D.R. conceived the experiments. M.B. designed and M.B., A.Y., O.Z., M.C. and N.K. performed experiments and collected data. E.R. analysed the lymphoid compartment of ribosomal protein heterozygote mice. P.H.R. designed, performed and interpreted CGH experiments. M.B. and D.R. analysed the data and wrote the manuscript.

Author Information Reprints and permissions information is available at www.nature.com/reprints. Correspondence and requests for materials should be addressed to M.B. (maria.barna@ucsf.edu) or D.R. (Davide.Ruggero@ucsf.edu).

METHODS

Mice. *Eμ-Myc*/+ transgenic mice, $L24^{+/-}$, $L38^{+/-}$ and $p53^{-/-}$ mice were all maintained on a C57/BL6 background and their offspring were bred in accordance with protocols approved by the committee for animal research at the University of California, San Francisco, to obtain the genotypic combinations described in this paper. In all cases, *Eμ-Myc*/+ transgenic mice were maintained and studied on a heterozygote background. Mice were monitored twice a week for signs of morbidity and tumour development. Myc tumour initiation was scored by peripheral lymph node palpation as previously described[31]. Moribund mice (*Eμ-Myc*/+, *Eμ-Myc*/+; $L24^{+/-}$, *Eμ-Myc*/+; $L38^{+/-}$, $p53^{-/-}$, $p53^{-/-}$;$L24^{+/-}$) or mice with obvious tumours were killed, and tumours and different organs were analysed by histology or processed for further analysis.

Cell culture and analysis of IRES dependent translation in mitosis. Primary B-lymphocytes were isolated from spleen or bone marrow from 4–5-week-old mice using an autoMACS separator (Miltenyi Biotec) according to the manufacturer's instructions. To synchronize primary B-lymphocytes in mitosis, 2×10^6 cells ml^{-1} were plated in culture medium (RPMI-1640 supplemented with 10% fetal bovine serum (FBS), 1% penicyllin/streptomycin, 0.5% β-mercaptoethanol, 5 μg ml^{-1} CD40 and 15 μg ml^{-1} IL-4). After 24 h, cells were resuspended in fresh culture medium supplemented with 2.5 mM thymidine and incubated for 18 h to arrest cells in S phase. Cells were released from the thymidine block by washing in PBS plus 2% FBS and incubated in fresh culture medium for 6 h. Thymidine (2.5 mM) was then added to the medium for 24 h. The cells were released from the second thymidine block as described above and incubated in fresh culture medium containing 1.5 μM nocodazole for 16 h to arrest cells in mitosis. Mouse embryonic fibroblasts (MEFs) were isolated from wild-type and $L24^{+/-}$13–14 days post coitum embryos and infected with MycER[32]. Cells were transfected at steady state and in mitosis. For the steady state condition, MEFs were plated in 6-well culture plates at $\sim 5 \times 10^5$ cells per well and allowed to grow overnight to ~50% confluency. Transfection and subsequent steps were performed concurrently in both steady state and mitosis. Synchronization in mitosis was performed as previously described[33]. In brief, after release from the aphidicolin block, MEFs were transfected with the HCV IRES or Cdk11^{p58} IRES RNA bicistronic vector as previously described[30]. At this time MycER was activated by the addition of OHT. Cells were collected 12 h in mitosis and Firefly and *Renilla* activities were quantified using the Glomax luminometer. Bicistronic messenger RNA levels were normalized by quantitative PCR (qPCR) using Rluc 5′-AACGCGGCCTCTTCTTATTT-3′; 5′-ATTTGCCTGATTTGCCCATA-3′ and Fluc 5′-GAGGTTCCATCTGCAGGTA-3′; 5′-CCGGTATCCAGATCCACAAC-3′ primers. IRES-dependent expression of endogenous Cdk11^{p58} was performed by western blot using rabbit polyclonal anti-CDK11^{p58} from Abcam. Expression of β-actin was detected to confirm equal loading.

Analysis of global protein synthesis. Equal numbers of freshly isolated or cultured primary B-lymphocytes (synchronized in S phase or mitosis) from 4–5-week-old mice were incubated in methionine-free DMEM for 45 min and then 50 μCi per well (25 μCi ml^{-1}) of [^{35}S] methionine (Perkin Elmer) was added to the cultures for 35 min. Whole cell lysates were prepared with protein extraction buffer (50 mM Tris-HCl, pH 7.5, 150 mM NaCl, 1 mM dithiothreitol, 1 mM EDTA, 1% Triton X-100, 1× protease inhibitor cocktails) by freezing in dry ice for 3 min and thawing at 37 °C for 3 min. Thirty micrograms of protein was loaded on a 4–20% Tris-HCl gradient gel (Bio-Rad) and transferred onto a nitrocellulose membrane. In certain experiments, cells were pretreated with 200 nM rapamycin (Sigma) and incubated for 45 min at 37 °C[34]. Thirty microcuries of ^{35}S was added to each well and incubated for 90 min at 37 °C. Radiolabelled proteins were visualized by exposure to X-ray film at −80 °C for 16 h. The radioactivity of each lane was quantified by densitometry analysis.

Cellular and molecular analysis of lymphocytes. Freshly isolated and cultured B-lymphocytes from 4–5-week-old mice were fixed in 95% ethanol, labelled with propidium iodide and cell cycle analysed using a BD Biosciences FACSCalibur system. For *in vivo* analysis of cell cycle rates, mice (4–6 weeks old) were administered 1 mg of BrdU (BD Biosciences BrdU Flow Kit) by intraperitoneal (i.p.) injection 6 h before being killed. Spleenocytes were washed with PBS containing 3% FBS and 0.09% NaN_3 and B-lymphocytes were labelled with pacific blue-conjugated rat-anti mouse B220 (BD Biosciences). BrdU staining was performed using the BD Biosciences BrdU Flow Kit following manufacturer's instructions. Samples were analysed using a BD Biosciences LSRII flow cytometer and the BD Biosciences FACSDiva software. The percentage of BrdU-positive B-lymphocytes was determined using the FlowJo 8.7.1 software. For the immunophenotypic analysis of blood and spleen from $L24^{+/-}$ and $L38^{+/-}$ mice, 100 μl of peripheral blood and splenic cell suspensions obtained by mechanical disruption of the spleen, were processed and stained with the following combination of monoclonal antibodies conjugated with FITC or PE: CD19-PE and CD3-FITC, CD4-PE and CD8-FITC, and CD43-PE and CD45R-B220-FITC. Fluorochrome-conjugated isotypic antibodies of irrelevant specificity were used as negative controls. Red blood cells were lysed immediately after labelling by incubation with 2 ml of FACS lysis solution (BD Biosciences) as recommended by the manufacturer. A minimum of 10,000 events per tube were acquired with a BD Biosciences LSRII flow cytometer. Mononuclear cells were gated and the percentage of each cell subset was determined using the CellQuest software (BD Biosciences). TUNEL assay (Roche) was performed on freshly isolated lymphocytes by following the manufacturer's instructions. Cell volume measurements were performed using a Coulter Model Z2 (Beckman Coulter). Cells were diluted in Isoton II (Beckman Coulter) at 100,000 cells ml^{-1} in 10 ml. A 1-ml sample was analysed according to the manufacturer's instructions. Fifty-thousand sorted cells were resuspended in 6 ml of Isoton II, and 1 ml was analysed. Centrosome analysis was performed on cell cytospins fixed in cold methanol for 10 min and then briefly incubated in ice-cold acetone. The antibodies used for immunofluorescence staining were anti-mouse γ-tubulin (T-6557 Sigma; 1:1,000) and 4,6-diamidino-2-phenylindole (DAPI). For western blot analysis total proteins were extracted in buffer A (150 mM NaCl, 20 mM NaH_2PO_4, 2 mM EGTA, 2 mM EDTA, 0.5 % Triton X-100, 1 mM dithiothreitol and Complete Protease Inhibitor Cocktail Tablets (Roche)), and 30 μg of proteins were used. The membrane was probed with the appropriate antibody; anti-mouse p27 (BD Biosciences), anti-rabbit cyclin D2 (Santa Cruz) and anti-mouse p21 (BD Biosciences). Expression of β-actin was detected to confirm equal loading.

CGH analysis. Genomic DNA extracted from lymphomas of six *Eμ-Myc*/+ transgenic mice and six *Eμ-Myc*/+;$L24^{+/-}$ mice was subjected to CGH array analysis. High-molecular-mass mouse DNA was extracted from mutant mice and normal tissue by standard methods and subjected to CGH according to the previously published method with some modifications[35]. In brief, the test DNA and reference DNA were labelled by nick-translation with fluorescein-12-dUTP and Texas Red-5-dUTP (NEN-DuPont), respectively. Equal amounts of test and reference DNA were coprecipitated along with 10 mg of mouse *Cot-1* DNA (GIBCO/BRL) and resuspended in the hybridization mix before *in situ* hybridization to mouse metaphase chromosome spreads on hybridization. The chromosomes were counterstained with DAPI to allow their identification. Then, 10 to 15 separate metaphases were captured for each case using a cooled charge-coupled devices (CCD) camera attached to a Nikon Eclipse 800 microscope. Copy number changes were detected on the basis of the variance of the red:green ratio profile from the standard of one. Ratio values of 1.20 and 0.80 were used as upper and lower thresholds to define gains and losses, respectively.

Cytokinesis analysis. A full-length $Cdk11^{p58}$ cDNA was generated from mitotically synchronized B cells using PCR with reverse transcription (RT–PCR) with the following primers: 5′-GAATTCTGAGGAAATGAGTGAAGATGAAGAC-3′ and 5′-GTCGACGACCTCAGAACTTGAGGCTGAA-3′. *p58* PITSLRE cDNA was cloned in retroviral pBABE construct harbouring hygromycin resistance. Primary MEFs were stably transfected with *MycER* harbouring puromycin resistance or with $Cdk11^{p58}$ cDNA plus *MycER* via a Phoenix viral vector and cultured in DMEM containing 10% FBS. Wild type, *MycER* and *p58;MycER* cells were each plated in chamber slides at 2×10^{-4} cells per well. Synchronization in mitosis was performed as previously described[33]. After release from aphidicolin, Myc was activated by the addition of OHT. At the 20 h time point, cells were fixed in 4% paraformaldehyde and stained with an antibody against α-tubulin (Sigma) and with DAPI. Binucleated cells were scored from more than four independent experiments with a minimal of 500 cell counts each. The slides were scanned using a motorized XY stage and acquired images were processed using the taxonomy features in Nikon Elements software V3 to quantify the number of binucleated cells for each well.

Semi-quantitative and quantitative RT–PCR. Total RNA from B-lymphocytes was extracted using Trizol (Invitrogen) and purified using RNeasy (Qiagen) following the manufacturer's instructions. From each sample, 3 μg RNA was treated with DNase (Turbo DNA Free, Ambion). Then, 1 μg was used for cDNA synthesis with the SuperScript III First-Strand Synthesis System (Invitrogen) following manufacturer's instructions and using 2.5 μg random primers (Promega), 0.5 mM dNTPs and 400 U SuperScript III in a reaction volume of 100 μl. From each sample, 1 μg RNA was used as negative control by the omission of reverse transcriptase. For PCR, 1/10 (v/v) of cDNA was used with 300 nM of the specific primers in a reaction volume of 25 μl. qPCR was used for the analysis of *p21* and *p27* expression. SYBR GREEN PCR Master Mix (Applied Biosystems) was used and the thermal profiles were: pre-denaturation for 10 min at 95 °C, followed by 42 cycles of denaturation at 95 °C for 20 s, annealing at 57 °C for 30 s and extension at 72 °C for 30 s. Reactions were performed in duplicate in an Applied Biosystems 7300 thermocycler and the 7300 software system v1.4.0 was used for analysis. At the end of each PCR reaction, dissociation curves were generated to verify the formation of a specific amplicon.

Primer sequences used were: *p21*, 5′-GACAGTGAGCAGTTGCG-3′, 5′-CTCAGACACCAGAGTGC-3′; *p27*, 5′-TCAAACGTGAGAGTGTCTAACGG-3′; *β-actin*, 5′-CCTAGCACCATGAAGATCAAG-3′, 5′-ATCGTACTCCTGCTTGCTG-3′. Forward and reverse primers used for *Gadd45a* qPCR were purchased from SuperArray (PPM02927B). As a positive control for cellular stress and induction of *Gadd45α* mRNA expression, 3T3 cells were incubated with 100 μg ml^{-1} methyl methanesulphonate in culture medium (DMEM, 10% FBS and 1% streptomycin/penicillin) for 4 h and total RNA was extracted using Trizol. Semi-quantitative PCR was used for the analysis of cyclin D2 expression. GoTaq Master Mix (Promega) was used and the thermal profiles were: predenaturation for 3 min at 94 °C, followed by 25 cycles (denaturation for 30 s at 94 °C, annealing for 30 s at 53 °C (for *cyclin D2*), and 57 °C (for *β-actin*), elongation for 1 min at 72 °C) and final elongation for 10 min at 72 °C. Primer sequences were: *cyclin D2*, 5′-GTTCTGCAGAACCTGTTGAC-3′, 5′-ACAGCTTCTCCTTTTGCTGG-3′; *β-actin*, 5′-GTATGGAATCCTGTGGCATC-3′, 5′-AAGCACTTGCGGT GCACGAT-3′. Amplicons were resolved in 1.5% agarose gel containing 40 mM Tris-acetate, 1 mM EDTA, pH 8.0, and 0.5 μg ml^{-1} ethidium bromide. Gels were photographed by ultraviolet transilumination using an AlphaInnotec camera and software. Relative expression ratios were obtained by densitometry using the ImageJ software.

31. Ruggero, D. L. *et al.* The translation factor eIF-4E promotes tumor formation and cooperates with c-Myc in lymphomagenesis. *Nature Med.* **10,** 484–486 (2004).
32. Lenahan, M. K. & Ozer, H. L. Induction of c-myc mediated apoptosis in SV40-transformed rat fibroblasts. *Oncogene* **12,** 1847–1854 (1996).
33. Ferguson, A. M., White, L. S., Donovan, P. J. & Piwnica-Worms, H. Normal cell cycle and checkpoint responses in mice and cells lacking Cdc25B and Cdc25C protein phosphatases. *Mol. Cell Biol.* **25,** 2853–2860 (2005).
34. Beretta, L., Gingras, A. C., Svitkin Y.V., Hall M. N. & Sonenberg, N. Rapamycin blocks the phosphorylation of 4E-BP1 and inhibits cap-dependent initiation of translation. *Embo J.* **15,** 658–664 (1996).
35. Kallioniemi, O. P. *et al.* Optimizing comparative genomic hybridization for analysis of DNA sequence copy number changes in solid tumors. *Genes Chromosom. Cancer* **10,** 231–243 (1994).